2008

Star Formation Rate Determinations

D Calzetti
University of Massachusetts - Amherst, calzetti@astro.umass.edu

FULL TITLE
ASP Conference Series, Vol. **VOLUME**, **YEAR OF PUBLICATION**
NAMES OF EDITORS

Star Formation Rate Determinations

Daniela Calzetti

Dept. of Astronomy, University of Massachusetts, Amherst, MA, U.S.A.

Abstract. I review determinations of star formation rate (SFR) indicators from the ultraviolet to the infrared, in the context of their use for galaxies and galaxy surveys. The mid-infrared SFR indicators have garnered interest in recent years, thanks to the Spitzer capabilities and the opportunities offered by the upcoming Herschel Space Telescope. I discuss what we have learned in the mid-infrared from studies of local galaxies combining Spitzer with HST and other data.

1. Introduction

Star formation is one of the fundamental processes driving the evolution of galaxies. It depletes galaxies of gas (and dust) by converting it to stars, controls the metal enrichment of the interstellar (ISM) and intergalactic medium (IGM), regulates the radiative and mechanical feedback into the ISM and IGM, and shapes the stellar populations' mix. Star formation is the true link between the invisible Universe (driven by gravity, and traced by models of galaxy formation and evolution, e.g., Katz 1992; Springel & Hernquist 2003; Springel, di Matteo & Hernquist 2005; Stinson et al. 2006) and the visible Universe that is typically measured, one example being the redshift evolution of the cosmic star formation rate density in comoving space (e.g., Madau et al. 1996; Lilly et al. 1996; Smail, Ivison & Blain 1997; Madau, Pozzetti & Dickinson 1998; Hughes et al. 1998; Steidel et al. 1999; Eales et al. 1999; Yan et al. 1999; Barger, Cowie & Richards 2000; Wilson et al. 2002; Giavalisco et al. 2004; Norman et al. 2004; Chapman et al. 2005; Hopkins & Beacom 2006). Thus, it becomes paramount to characterize and physically quantify the laws of star formation (Kennicutt 1998a; Kennicutt et al. 2007), and to obtain accurate measures of the star formation rates of galaxies.

Star formation rates indicators have been defined at, basically, all wavelengths across the spectrum, from the X–ray to the radio (see, e.g., Kennicutt 1998b; Kewley et al. 2002; Ranalli, Comastri & Setti 2003; Bell 2003; Hopkins 2004; Kewley, Geller & Jansen 2004; Calzetti et al. 2005; Schmitt et al. 2006; Calzetti et al. 2007, and references therein). The common characteristic of all indicators is that they all probe the *massive stars formation rate*. To convert this measure to a SFR, an assumption on the stellar Initial Mass Function (IMF) needs to be made; this problem is being covered in other presentations at this conference, together with the stochastic effects present at low star formation levels (see, e.g., P. Kroupa's contribution to this conference).

This review mostly concentrates on the robustness of converting the luminosity $L(\lambda)$ of a whole galaxy into a SFR indicator, and the potential impact of contributions to $L(\lambda)$ that are not strictly linked to the current star forma-

tion. Examples of such 'extraneous' contributions are evolved stellar populations, which may contribute to the light emitted at a given wavelength but are not part of the star–forming population, or the presence of dust.

For sake of brevity, I will only touch upon SFR indicators at ultraviolet (UV), optical, and infrared (FIR) wavelengths. Indicators at UV and optical/near–infrared indicators only probe the stellar light that emerges from galaxies *unabsorbed by dust*. Infrared SFR indicators are complementary to UV–optical indicators, because they measure star formation via the stellar light that has been reprocessed by dust and emerges beyond a few μm.

2. The Ultraviolet

The ultraviolet (λ ∼912–3000 Å) emission from galaxies is extensively used as a SFR indicator, especially in the medium/high redshift regime, where the rest-frame UV moves into the optical observer's frame. Recently, GALEX (Martin et al. 2005), with its UV survey capability, has revamped the interest of this wavelength regime for studies in the local Universe (e.g., Salim et al. 2007).

The advantage of using the UV is that it directly probes the bulk of the emission from young, massive stars. Its main disavantage, however, is its high sensitivity to dust reddening and attenuation. For reference, a star–forming galaxy with A_V=1 mag has $A_{1500\ \mathring{A}} \approx 3$ mag, but the specific value will depend on both the dust amount *and* the dust geometry in the galaxy. To make matters worse, there is a well–established correlation between attenuation and SFR in galaxies and star–forming regions (Figure 1, Wang & Heckman 1996; Heckman et al. 1998; Calzetti 2001; Hopkins et al. 2001; Sullivan et al. 2001; Buat et al. 2002; Calzetti et al. 2007); thus, the galaxies that are most actively forming stars and are, therefore, likely to be important in the cosmic SFR census, are also those whose UV luminosity requires the largest corrections for the effects of dust attenuation. An increase of a factor 100 in SFR implies on average an increase in the attenuation by $A_V \approx$1–3 mag, for star–forming galaxies. The quantitative details may depends on the exact nature of the star–forming system, but the qualitative trend is common to most (Figure 1). At fixed metallicity (and dust–to–gas ratio, Draine et al. 2007), this trend is a consequence of the correlation between SFR density and gas density (Kennicutt 1998a; Kennicutt et al. 2007). A number of authors (e.g., Calzetti, Kinney & Storchi–Bergmann 1994; Meurer, Heckman & Calzetti 1999; Calzetti et al. 2000; Hopkins et al. 2001; Sullivan et al. 2001; Buat et al. 2002, 2005; Bell 2003; Hopkins 2004; Iglesias–Paramo et al. 2006; Salim et al. 2007) have derived techniques to correct the observed UV emission from galaxies for the effects of dust attenuation. The effectiveness of these techniques, however, depends in general on the nature of the galaxy population they are being applied to.

The additional complication with using the UV as a SFR indicator is the long timescale (of–order 100 Myr) in which stars are relatively luminous in the non–ionizing UV wavelength range. The cross–calibration of SFR(UV) with indicators at other wavelengths may be complicated by the different timescales involved. This may be the case when comparing SFR(UV) with, e.g., SFR(Hα) (see next section), where the latter has a timescale about 10 times shorter than

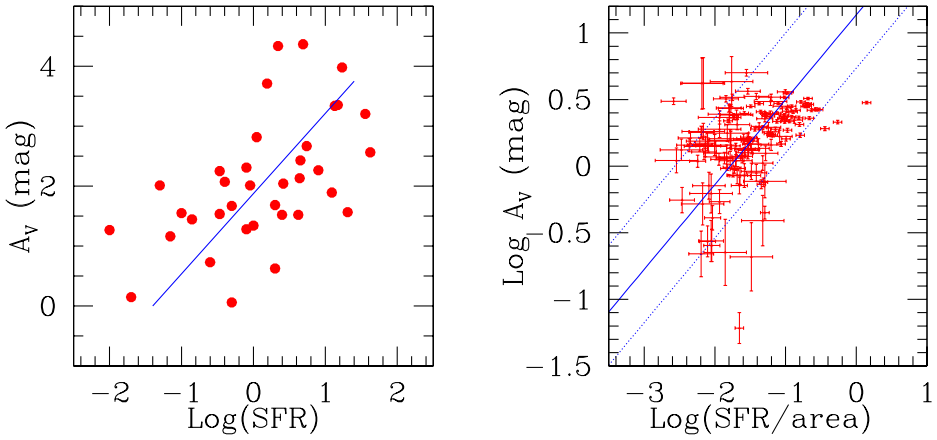

Figure 1. **Left.** The attenuation A_V (in magnitudes), derived from hydrogen nebular line emission (Hα/Hβ or Hβ/Brγ, Calzetti, Kinney & Storchi–Bergmann 1996) as a function of the log(SFR) (in units of $M_\odot$ yr^{-1}) for a sample of local starbursts; the continuous line shows the mean trend of the datapoints. **Right.** As similar plot to the one at left (but in log–log scale), this time for 164 star–forming regions in 21 nearby galaxies. All the galaxies have metallicity close to the solar value. A_V (from the Hα/Pα ratio) is in units of magnitudes, and the SFR density in the horizontal axis is in units of $M_\odot$ yr^{-1} kpc^{-2}. The continuous line is the expected trend after combining the Schmidt–Kennicutt law with the dust–to–gas ratio of the galaxies (Calzetti et al. 2007). The dotted lines are the 90% boundary to the datapoints.

the former. In this case, the star formation history of the system plays a significant role. If an unresolved object is only measured, say, at 1500 Å, it will be impossible to know whether the emission is coming from a system that has been forming stars at the constant level of 1 $M_\odot$ yr^{-1} for the past 100 Myr, or a system that is no longer forming stars but has been passively evolving for the past 50 Myr after a 4×10^8 $M_\odot$ burst of star formation (Leitherer et al. 1999).

The ≈10 times longer stellar timescales probed by the UV relative to tracers of ionizing photons accounts for the difference in the properties of the dust attenuation between starburst and quiescent star–forming systems. Starburst galaxies show a well–defined correlation in the FIR/UV–versus–UV color plane (Figure 2 Meurer, Heckman & Calzetti 1999). The FIR/UV ratio is a measure of the UV attenuation suffered by the system: the higher the dust attenuation, the larger the amount of UV stellar energy reprocessed into the FIR by dust. Variations in the UV color probe the amount of dust reddening present in the system. Thus, in starbursts, the UV reddening is a good tracer of the total UV dust attenuation (Calzetti 2001). Quiescent star–forming galaxies and regions show a ∼10 times larger spread in the FIR/UV ratio than starburst galaxies, at fixed UV color; the spread is in the sense that the starburst galaxies form the upper envelope to the quiescently star–forming systems (Figure 2 and Buat et al. 2002, 2005; Bell et al. 2002; Gordon et al. 2004; Kong et al. 2004; Seibert et al. 2005; Calzetti et al. 2005). Thus, a far larger range of UV dust attenuations

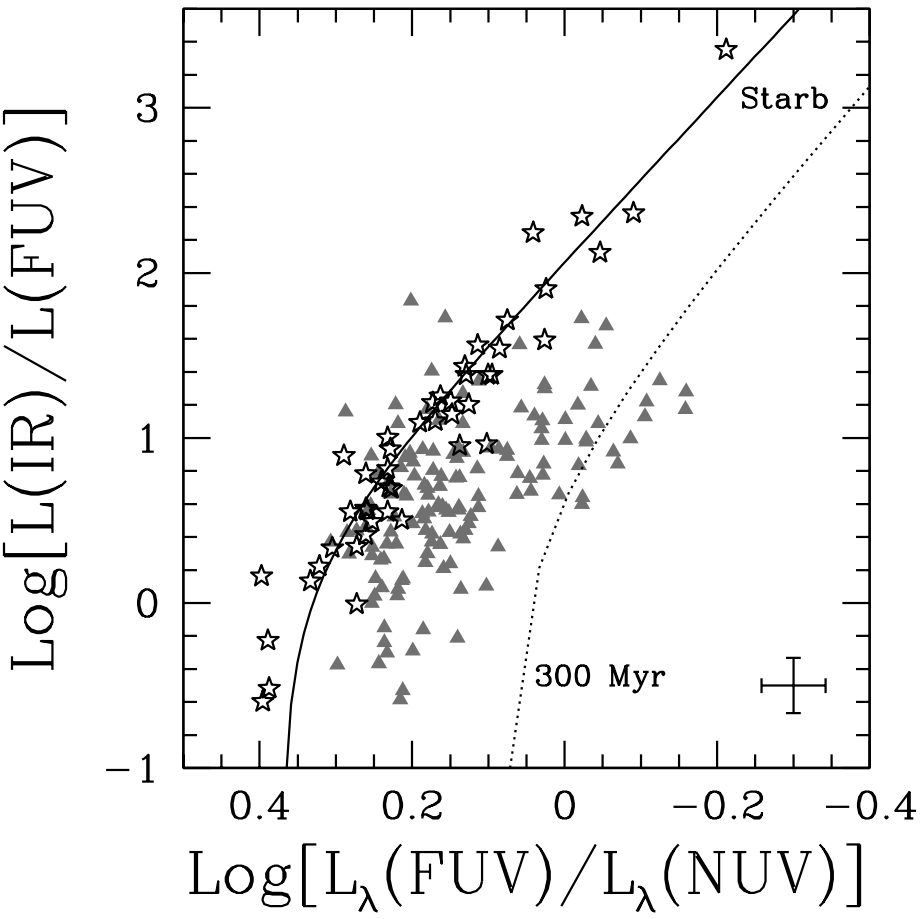

Figure 2. The FIR/UV ratio (the ratio of the far–infrared to the far–UV luminosity) versus the UV color (given here as the ratio between the GALEX far–UV and near–UV fluxes) for starburst galaxies and quiescently star–forming regions. The starburst galaxies are shown with star symbols. The grey filled triangles are star–forming regions within the galaxy NGC5194 (Calzetti et al. 2005). Redder UV colors correspond on average to larger FIR/UV ratios. The continuous line shows the best fit to the starburst galaxies, which is well represented by a model of a progressively more attenuated (from left to right) constant star–forming population. The dotted line shows the same dust attenuation trend for a 300 Myr old stellar population; this model represents a reasonable lower envelope to the NGC5194 star–forming regions.

seems to be present in star–forming objects than in starbursts, for the same UV color. This is possible if in quiescent star–forming systems the reddening of the UV colors is not only a probe of dust, but also of ageing of the individual star–forming regions contributing to the UV emission in the system (regions up to an age of ≈100–300 Myr, Calzetti et al. 2005). Specifically, older clusters can contribute significantly to the measured UV emission in these galaxies, as they

are not as attenuated by dust as younger systems. This will complicate the definition of SFR(UV) in quiescent star–forming galaxies, and change its calibration relative to the starburst galaxies (e.g., Seibert et al. 2005; Cortese et al. 2006; Salim et al. 2007).

3. The Optical and Near–Infrared

SFR indicators in the optical and near–infrared wavelength range (λ ∼3000–25,000 Å) are derived from the many hydrogen recombination lines (mainly Hα, Hβ, Pβ, Pα, Brγ) and from forbidden line emission (chiefly [OII] and [OIII]). These indicators, thus, trace the ionizing photons in the system. The short lifespan of massive, ionizing stars confines the timescale probed by the optical indicators to about 10 Myr, implying that they are tracers of the *current* SFR.

Calibrations for these indicators, in particular for Hα(λ6563 Å) and for [OII](λ3727 Å), have been presented by many authors (to name a few, Kennicutt 1998b; Gallagher, Hunter & Bushouse 1989; Jansen, Franx & Fabricant 2001; Rosa–Gonzalez, Terlevich & Terlevich 2002; Kewley et al. 2002; Charlot & Longhetti 2001; Kewley, Geller & Jansen 2004; Moustakas, Kennicutt & Tremonti 2006, and references therein).

There are a number of effects that impact the SFRs derived from optical and near–infrared line emission. First and foremost, dust extinction, which affects the blue lines more than the red ones. For example, if extinction corrections are neglected, the median SFR derived for a generic sample of nearby galaxies will be underestimated by roughly a factor of 3 if using Hα, and by about twice as much if using [OII] (Rosa–Gonzalez, Terlevich & Terlevich 2002). These mean values do not convey the fact that brighter galaxies are also more extincted, as discussed in the previous section. In starburst galaxies, dust attenuation is about a factor of two larger for the ionized gas than for the stellar continuum, at the same wavelength (Calzetti, Kinney & Storchi–Bergmann 1994): the dust attenuation in the Hβ(λ4861 Å) line is the same that in the stellar continuum at ∼2300 Å.

Line emission SFR indicators are also sensitive to the upper end of the stellar IMF, i.e., the number of ionizing stars formed, much more than the UV stellar continuum. Changing the upper stellar mass of the IMF from 100 $M_\odot$ to 30 $M_\odot$ decreases the number of ionizing photons by a factor of ∼5, and the UV stellar continuum at 1500 Å by a factor 2.3 (from the models of Leitherer et al. 1999). Other factors to take into account for the line emission SFR indicators are the underlying stellar absorption in the case of the hydrogen recombination lines (Rosa–Gonzalez, Terlevich & Terlevich 2002), and the metallicity and ionization conditions for the forbidden lines (e.g., Moustakas, Kennicutt & Tremonti 2006).

For reference, for a solar metallicity stellar population with constant SFR over the past 100 Myr, forming stars with an IMF consisting of two power laws, with slope −1.3 in the range 0.1–0.5 $M_\odot$ and slope −2.3 in the range 0.5–120 $M_\odot$, the SFR(Hα) is given by:

$$SFR(M_\odot\ yr^{-1}) = 5.3 \times 10^{-42} L(H\alpha)(erg\ s^{-1}). \quad (1)$$

Variations of ±20% on the calibration in this relation are present for younger/older ages and metallicities down to ∼1/5th solar. The ∼50% difference between the calibration in Equation 1 and that of Kennicutt (1998b) is mainly due to differences in assumptions on the stellar IMF and the age of the stellar populations (100 Myr in our case versus infinite age in Kennicutt (1998b)).

4. The Infrared

The earliest calibrations of the infrared (λ ∼5–1000 μm) dust emission as a SFR indicator date back to IRAS (see, for a review and an independent calibration, Kennicutt 1998b). The connection between star formation and infrared emission is based on the fact that, at least in the nearby Universe, star–forming regions tend to be dusty and the dust absorption cross–section peaks in the UV (also the peak of emission of young, massive stars).

Since the very beginning, however, it was clear that the calibration of the FIR emission as a SFR tracer carried a number of issues (Hunter et al. 1986; Lonsdale Persson & Helou 1987; Rowan–Robinson & Crawford 1989; Devereux & Young 1990; Sauvage & Thuan 1992). First, not all of the luminous energy produced by recently formed stars is re-processed by dust in the infrared; in this case, the FIR only recovers part of the SFR, and the fraction recovered depends, at least partially, on the amount of dust in the system. Second, evolved, i.e., non-star-forming, stellar populations also heat the dust that emits in the FIR wavelength region, thus affecting the calibration of SFR(FIR) in a stellar-population-dependent manner. Third, SFR(FIR) is a 'calorimetric' measure (the full energy census in the range ∼5–1000 μm needs to be included), and the FIR spectral energy distribution (SED) depends on the stellar field intensity (Helou 1986; Draine & Li 2006); thus, extrapolations of SFR(FIR) from too a sparsely sampled SED are subject to large uncertainties.

The use of monochromatic (i.e., one band or wavelength) infrared emission for measuring SFRs offers one definite advantage over the bolometric infrared luminosity: it removes the need for uncertain extrapolations of the dust SED across the full wavelength range. The interest in calibrating monochromatic mid-infrared SFR diagnostics stems from their potential application to both the local Universe (e.g., in the investigation of the scaling laws of star formation Kennicutt et al. 2007) and intermediate and high redshift galaxies observed with Spitzer, Herschel and future millimiter/radio facilities (e.g. Daddi et al. 2005; Wu et al. 2005).

Studies using ISO data provided the first window on the use of the monochromatic mid–IR (MIR, λ ∼5–40 μm) emission as a SFR indicator; investigations with the higher angular resolution and more sensitive Spitzer 8 μm and 24 μm data have expanded on the ISO results. The dust emission in the MIR wavelength range is characterized by both continuum and bands. The continuum is due to dust heated by a combination of single–photon and thermal equilibrium processes, with the latter becoming more and more prevalent over the former at longer wavelengths (Draine & Li 2006). The interest in calibrating the MIR dust continuum as a SFR indicator stems from the consideration that the dust heated by hot, massive stars can have high temperatures and will then emit at short infrared wavelengths. The MIR bands are generally attributed to Polycyclic Aro-

matic Hydrocarbons (PAH, Leger & Puget 1984; Sellgren 1984), large molecules transiently heated by single UV and optical photons in the general radiation field of galaxies or near B stars (Li & Draine 2002; Peeters, Spoon & Tielens 2004; Mattioda et al. 2005), and which can be destroyed, fragmented, or ionized by harsh UV photon fields (Boulanger et al. 1988; Pety et al. 2005).

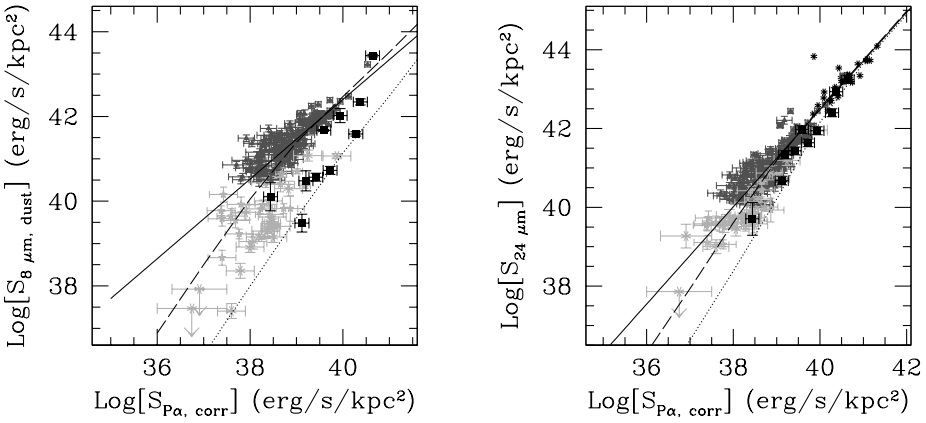

Figure 3. **Left.** The luminosity surface density (LSD=luminosity/area) at 8 μm versus the Pα LSD of 10 starburst galaxies and 220 star–forming regions in 33 nearby galaxies (Calzetti et al. 2007). The 8 μm emission is from Spitzer images, and has the stellar continuum subtracted. The Pα line emission (λ=1.876 μm) is from HST/NICMOS images, has been corrected for dust extinction using the Hα/Pα ratio, and is used here as an unbiased tracer of massive stars SFR. Of the 220 regions, the $\sim$180 regions in high–metallicity galaxies, 12+log(O/H)>8.3, are marked in dark grey, and the $\sim$40 regions in low–metallicity galaxies are in light grey. The starburst galaxies (Engelbracht et al. 2005) are the black squares. The continuous line is the best fit to the high–metallicity star–forming regions (dark grey), and has slope 0.94. Models for a young stellar population with increasing amount of star formation and dust are shown as a dash line (Z=Z$_\odot$) and a dot line (Z=1/10 Z$_\odot$), using the stellar population models of Leitherer et al. (1999) and the dust models of Draine & Li (2006). The spread in the datapoint around the best fit line is well accounted for by a spread in the stellar population's age in the range 2–8 Myr. **Right** The same as a left panel, with the vertical axis now reporting the 24 μm LSD, also from Spitzer. The black asterisks are the Luminous Infrared Galaxies (LIRGS) from Alonso–Herrero et al. (2006). The best fit line (continuous line) has slope 1.2.

Roussel et al. (2001) and Förster Schreiber et al. (2004) showed that the emission in the 6.75 μm ISO band correlates with the number of ionizing photons in galaxy disks and in the nuclear regions of galaxies. Conversely, Boselli, Lequeux & Gavazzi (2004) found that the mid–IR emission in a more diverse sample of galaxies (types Sa through Im–BCDs) correlates more closely with tracers of evolved stellar populations not linked to the current star formation. Additionally, Haas, Klaas & Bianchi (2002) found that the ISO 7.7 μm emission is correlated with the 850 μm emission from galaxies, suggesting a close relation between the ISO band emission and the cold dust heated by the general (non–star–forming) stellar population.

Spitzer data of the nearby galaxies NGC300 and NGC4631 show that the 8 μm band emission highlights the rims of HII regions and is depressed inside the regions, indicating that the PAH dust is heated in the photo–dissociation regions surrounding HII regions and is destroyed within the regions (Helou et al. 2004; Bendo et al. 2006). Analysis of the mid–IR emission from the First Look Survey galaxies shows that the correlation between the 8 μm band emission and tracers of the ionizing photons is shallower than unity (Wu et al. 2005), in agreement with the correlations observed for HII regions in the nearby star–forming galaxy NGC5194 (Calzetti et al. 2005).

A recent analysis of the 8 μm emission from 220 star–forming regions in 33 nearby galaxies from the project SINGS (the Spitzer Infrared Nearby Galaxies Survey Kennicutt et al. 2003) has shown that this MIR band is sensitive to both metallicity and star formation history (Figure 3 left, and Calzetti et al. 2007). The dependence on metallicity (e.g., Boselli, Lequeux & Gavazzi 2004; Engelbracht et al. 2005; Draine et al. 2007) implies that regions with values about 1/10 $Z_{\odot}$ are about 30 times underluminous at 8 μm relative to regions with solar metallicity and same SFR. The dependence on star formation history is due to the contribution to the 8 μm emission from dust heated by non–ionizing stellar populations that are unrelated to the current star formation (Peeters, Spoon & Tielens 2004; Calzetti et al. 2007). However, for a restricted choice of parameters, i.e., actively star–forming regions with similar (e.g., solar) metallicity, the 8 μm emission correlates almost linearly with the SFR (Figure 3, left).

The same analysis shows that the 24 μm emission is, conversely, a good SFR tracer for galaxies, in the absence of strong AGNs (Figure 3, right, and Calzetti et al. 2007). Similar conclusions had been reached by Calzetti et al. (2005) and by Perez–Gonzalez et al. (2006) for star–forming regions in NGC5194 and NGC3031, respectively, and by Wu et al. (2005) and Alonso–Herrero et al. (2006) for bright galaxies. In particular, Calzetti et al. (2005) has concluded that the 24 μm emission is more closely related to the Hα (ionizing photons) emission than to the UV (non–ionizing stellar continuum) emission. A single correlation can be defined over 3.5 orders of magnitude in luminosity surface density (luminosity/area), yielding the following SFR calibration:

$$SFR(M_{\odot}\ yr^{-1}) = 1.24 \times 10^{-38} [L(24\ \mu m)\ (erg\ s^{-1})]^{0.88}. \qquad (2)$$

This calibration is very similar to that of Alonso–Herrero et al. (2006), who have used a sample of Ultraluminous Infrared Galaxies, LIRGs, and NGC5194. The non–linear trend of L(24 μm) with SFR is a direct consequence of the increasing dust temperature for more actively star forming objects (Draine & Li 2006); higher dust temperatures correspond to higher fractions of the dust emission emerging in the MIR.

The 24 μm emission has a much lower sensitivity to metallicity than the 8 μm emission, decreasing by just a factor 2-4 for a tenfold decrease in metallicity. This small decrease if fully accounted by the increased transparency (lower dust–to–gas ratio) of the medium for lower metal abundances (Draine et al. 2007). In addition, there seem to be very little contribution to the 24 μm emission from non–ionizing stellar populations, at least within the limits of the Calzetti et al. (2007) analysis.

The sensitivity of the SFR indicator to variations in the dust content of the system can be removed by combining two tracers: one that probes the dust–obscured star formation and one that probes the unobscured one. Combining the 24 μm luminosity with the *observed* Hα luminosity (Figure 4) yields a new SFR indicator, with calibration (Kennicutt et al. 2007; Calzetti et al. 2007):

$$SFR(M_{\odot}\ yr^{-1}) = 5.3 \times 10^{-42}[L(H\alpha)_{obs} + (0.031 \pm 0.006)L(24\ \mu m)], \quad (3)$$

from equation 1. The calibration in equation 3 is unaffected not only by metallicity variations (Figure 4), but also by stellar population mix. However, it shows some deviation from a simple, linear correlation at high luminosity surface densities (Figure 4, and Calzetti et al. 2007), which simply reflects the non–linear trend of L(24 μm) with SFR once luminosities are sufficiently high that the infrared emission dominates over the line emission.

5. Summary

The SFRs based on the UV stellar continuum and the optical/near–infrared line emission probe the stellar light that emerges from a galaxy unabsorbed by dust. They both require corrections for the effects of dust, which can change the mean values of local samples by factors of few. In addition, comparisons of calibrations between SFR(UV) and SFR(line) require care, as the former probes stellar timescales that are at least an order of magnitude longer than the latter.

In the infrared, the calorimetric SFR(FIR) is based on measuring the stellar energy re–processed by dust and suffers from difficult–to–quantify contributions from non–star–forming stellar populations. Often SFR(FIR) needs to be extrapolated from sparse wavelength sampling, due to observational limitations, which leads to uncertainties.

Monochromatic mid–infrared SFR indicators offer a valid complement to the stellar–based SFR tracers and to SFR(FIR). SFR(MIR) tend to be more closely associated to the regions of ionizing photon emission than to regions of UV emission. In the absence of AGNs, L(24 μm) and a linear combination of L(Hα) and L(24 μm) provide relatively robust SFR tracers, with uncertainties of–order a factor 2. Conversely, the 8 μm emission is strongly dependent on both variations in metallicity (factor of 30 variation in luminosity for a factor $\sim$10 variation in metallicity) and in stellar population mix (factor of a few variation in luminosity). Equations 2 and 3 should be generally applicable to regions and galaxies dominated by current star formation.

Acknowledgments. This work would not have been possible without the combined efforts of the SINGS (Spitzer Infrared Nearby Galaxies Survey) team, whom the author thanks heart-fully. Special thanks are due to the SINGS project's Principal Investigator, Robert Kennicutt, and collaborators Chad Engelbracht, Bruce Draine, and Fabian Walter.

The author is grateful to Johan Knapen for all his excellent efforts in organizing this stimulating conference, and to John Beckman for offering the perfect excuse for it.

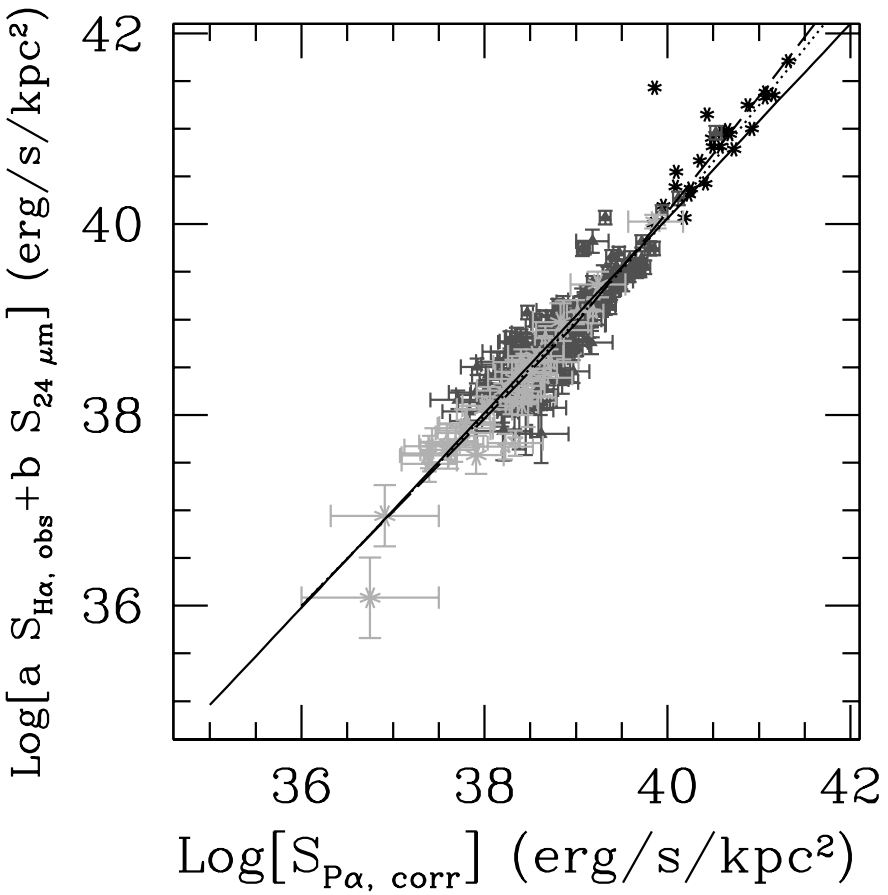

Figure 4. As in Figure 3, for the combined Hα and 24 μm LSD. For this SFR indicator, data and models are degenerate in metallicity. The slope of the best fit line is unity, and the data follow the 1–to–1 line up to the LIRGs. For the brightest galaxies, however, there are deviations from this trend, reflecting the increasing temperature of the dust in a regime where the 24 μm emission (i.e., the dust–obscured SFR) dominates over the Hα emission (the unobscured SFR).

References

Alonso–Herrero, A., Rieke, G.H., Rieke, M.J., Colina, L., Perez-Gonzalez, P.G., & Ryder, S.D. 2006, ApJ, 650, 835
Barger, A.J., Cowie, L.L., & Richards, E.A. 2000, AJ, 119, 2092
Bell, E.F. 2003, ApJ, 586, 794
Bell, E.F., Gordon, K.D., Kennicutt, R.C., & Zaritsky, D. 2002, ApJ, 565, 994
Bendo, G.J., Dale, D.A., Draine, B.T., Engelbracht, C.W., Kennicutt, R.C., Calzetti, D., Gordon, K.D., Helou, G., Hollenbach, D., Li, AIgen, Murphy, E.J., et al. 2006, ApJ, 652, 283
Boselli, A., Lequeux, J., & Gavazzi, G. 2004, A&A, 428, 409

Boulanger, F., Beichmann, C., Desert, F.–X., Helou, G., Perault, M., & Ryter, C. 1988, ApJ, 332, 328
Buat, V., Boselli, A., Gavazzi, G., & Bonfanti, C. 2002, A&A, 383, 801
Buat, V., Iglesias-Paramo, J., Seiber, M., Burgarella, D., Charlot, S., Martin, D.C., Xu, C.K., Heckman, T.M.,, Boissier, S., Boselli, A., et al. 2005, ApJ, 619, L51
Calzetti, D. 2001, PASP, 113, 1449
Calzetti, D., Armus, L., Bohlin, R.C., Kinney, A.L., Koornneef, J., & Storchi-Bergmann, T. 2000, ApJ, 533, 682
Calzetti, D., Kennicutt, R.C., Bianchi, L., Thilker, D.A., Dale, D.A., Engelbracht, C.W., Leitherer, C., Meyer, M.J., et al. 2005, ApJ, 633, 871
Calzetti, D., Kennicutt, R.C., Engelbracht, C.W., Leitherer, C., Draine, B.T., Kewley, L., Moustakas, J., Sosey, M., et al. 2007, ApJ, in press (astroph/0705.3377)
Calzetti, D., Kinney, A.L., & Storchi–Bergmann, T. 1994, ApJ, 429, 582
Calzetti, D., Kinney, A.L., & Storchi–Bergmann, T. 1996, ApJ, 458, 132
Chapman, S.C., Blain, A.W., Smail, I., & Ivison, R.J. 2005, ApJ, 622, 772
Charlot, S., & Longhetti, M. 2001, MNRAS, 323, 887
Cortese, L., Boselli, A., Buat, V., Gavazzi, G., Boissier, S., Gil de Paz, A., Seibert, M., Madore, B.F., & Martin, D.C. 2006, ApJ, 637, 242
Daddi, E., Dickinson, M., Chary, R., Pope, A., Morrison, G., Alexander, D.M., Bauer, F.E., Brandt, W.N., Giavalisco, M., Ferguson, H., Lee, K.-S., Lehmer, B.D., Papovich, C., & Renzini, A. 2005, ApJ, 631, L13
Desert, F.–X., Boulanger, F., & Puget, J.L. 1990, A&A, 237, 215
Devereux, N.A., & Young, J.S. 1990, ApJ, 350, L25
Draine, B.T., & Li A. 2007, ApJ, 657, 810.
Draine, B.T., Dale, D.A., Bendo, G., Gordon, K.D., Smith, J.D.T., Armus, L., Engelbracht, C.W., Helou, G., Kennicutt, R.C., Li, A., et al. 2007, ApJ, accepted (astroph/073213)
Eales, S., Lilly, S., Gear, W., Dunne, L., Bond, J.R., Hammer, F., Le Fevre, O., & Crampton, D. 1999, ApJ, 515, 518
Engelbracht, C.W., Gordon, K.D., Rieke, G.H., Werner, M.W., Dale, D.A., & Latter, W.B. 2005, ApJ, 628, 29
Förster Schreiber, N.M., Roussel, H., Sauvage, M., & Charmandaris, V., 2004, A&A, 419, 501
Gallagher, J.S., Hunter, D.A., & Bushouse, H. 1989, AJ, 97, 700
Giavalisco, M., et al. 2004, ApJ, 600, L103
Gordon, K.D., Perez–Gonzalez, P.G., Misselt, K.A., Murphy, E.J., Bendo, G.J., Walfer, F., Thornely, M.D., Kennicutt, R.C., et al. 2004, ApJS154, 215
Haas, M., Klaas, U., & Bianchi, S. 2002, A&A, 385, L23
Heckman, T.M., Robert, C., Leitherer, C., Garnett, D.R., & van der Rydt, F. 1998, ApJ, 503, 646
Helou, G. 1986, ApJ, 311, L33
Helou, G., Roussel, H., Appleton, P., Frayer, D., Stolovy, S., Storrie–Lombardi, L., Hurst, R., Lowrance, P., et al. 2004, ApJS, 154, 253
Hopkins, A.M. 2004, ApJ, 615, 209
Hopkins, A.M., & Beacom, J.F. 2006, ApJ, 651, 142
Hopkins, A. M., Connolly, A. J., Haarsma, D. B., & Cram, L. E. 2001, AJ, 122, 288
Hughes, D.H., Serjeant, S., Dunlop, J., Rowan-Robinson, M., Blain, A., Mann, R.G., Ivison, R. Peacock, J., Efstathiou, A., Gear, W., et al. 1998, Nature, 394, 241
Hunter, D.A., Gillett, F.C., Gallagher, J.S., Rice, W.L., & Low, F.J. 1986, ApJ, 303, 171
Iglesias–Paramo, J., et al. 2006, ApJS, 164, 38
Jansen, R.A., Franx, M., & Fabricant, D. 2001, ApJ, 551, 825
Katz, N. 1992, ApJ, 391, 502
Kennicutt, R.C. 1998a, ApJ, 498, 541
Kennicutt, R.C. 1998b, ARA&A, 36, 189

Kennicutt, R.C., Armus, L., Bendo, G., Calzetti, D., Dale, D.A., Draine, B.T., Engelbracht, C.W., Gordon, D.A., et al. 2003a, PASP, 115, 928
Kennicutt, R.C., Calzetti, D., et al. 2007, ApJ, submitted
Kewley, L.J., Geller, M.J., Jansen, R.A., & Dopita, M.A. 2002, AJ, 124, 3135
Kewley, L.J., Geller, M.J., & Jansen, R.A. 2004, AJ, 127, 2002
Kong, X., Charlot, S., Brinchmann, J., & Fall, S.M. 2004, MNRAS, 349, 769
Leger, A., & Puget, J.L. 1984, A&A, 137, L5
Leitherer, C., Schaerer, D., Goldader, J.D., González Delgado, R.M., Robert, C., Kune, D.F., de Mello, D.F., Devost, D., & Heckman, T.M. 1999, ApJS, 123, 3
Li, A., & Draine, B.T. 2002, ApJ, 572, 762
Lilly, S. J., Le Fvre, O., Hammer, F., & Crampton, D. 1996, ApJ, 460, L1
Lonsdale Persson, C.J., & Helou, G.X. 1987, ApJ, 314, 513
Madden, S.C., Galliano, F., Jones, A.P., & Sauvage, M. 2006, A&A, 446, 877
Madau, P., Ferguson, H.C., Dickinson, M.E., Giavalisco, M., Steidel, C.C., & Fruchter, A. 1996, MNRAS, 283, 1388
Madau, P., Pozzetti, L., & Dickinson, M.E. 1998, ApJ, 498, 106
Martin, D.C., Fanson, J., Schiminovich, D., Morrissey, P., Friedman, P.G., Barlow, T.A., Conrow, T., Grange, R., Jelinsky, P.N., et al. 2005, ApJ, 619, L1
Mattioda, A.L., Allamandola, L.J., & Hudgins, D.M. 2005, ApJ, 629, 1183
Meurer, G.R., Heckman, T.M., & Calzetti, D. 1999, ApJ, 521, 64
Moustakas, J., Kennicutt, R.C., & Tremonti, C.A. 2006, ApJ, 642, 775
Norman, C., et al. 2004, ApJ, 607, 721
Peeters, E., Spoon, H.W.W., & Tielens, A.G.G.M. 2004, ApJ, 613, 986
Perez–Gonzalez, P.G., Kennicutt, R.C., Gordon, K.D., Misselt, K.A., Gil de Paz, A., Engelbracht, C.W., Rieke, G.H., Bendo, G.J., Bianchi, L., Boissier, S., Calzetti, D., Dale, D.A., et al. 2006, ApJ, 648, 987
Pety, J., Teyssier, D., Fosse‘, D., Gerin, M., Roueff, E., Abergel, A., Habart, E., & Cernicharo, J. 2005, A&A, in press (astroph/0501339)
Ranalli, P., Comastri, A., & Setti, G. 2003, A&A, 399, 39
Rosa–Gonzalez, D., Terlevich, E., & Terlevich, R. 2002, MNRAS, 332, 283
Roussel, H., Sauvage, M., Vigroux, L., & Bosma, A. 2001, A&A, 372, 427
Rowan–Robinson, M., & Crawford, J. 1989, MNRAS, 238, 523
Salim, S., Rich, M.R., Charlot, S., Brinchmann, J., Johnson, B.D., Schminovich, D., Seibert, M., Mallery, R., Heckman, T.M., Forster, K., et al. 2007, ApJS, in press (astroph/0704.3611)
Sauvage, M., & Thuan, T.X. 1992, ApJ, 396, L69
Schmitt, H.R., Calzetti, D., Armus, L., Giavalisco, M., Heckman, T.M., Kennicutt, R.C., Leitherer, C., & Meurer, G.R. 2006, ApJ, 643, 173
Seibert, M. et al. 2005, ApJ, 619, L55
Sellgren, K. 1984, ApJ, 277, 623
Smail, I., Ivison, R.J., & Blain, A.W. 1997, ApJ, 490, L5
Springel, V., & Hernquist, L. 2003, MNRAS, 339, 289
Springel, V., di Matteo, T. & Hernquist, L. 2005, MNRAS, 361, 776
Steidel, C.C., Adelberger, K.L., Giavalisco, M., Dickinson, M., & Pettini, M. 1999, ApJ, 519, 1
Stiinson, G., Seth, A., Katz, N., Wadsley, J., Governato, F., Quinn, T. 2006, MNRAS, 373, 1074
Sullivan, M., Mobasher, B., Chan, B., Cram, L., Ellis, R., Treyer, M., & Hopkins, A. 2001, ApJ, 558, 72
Wang, B., & Heckman, T.M. 1996, ApJ, 457, 645
Wilson, G., Cowie, L.L., Barger, A.J., & Burke, D.J. 2002, AJ, 124, 1258
Wu, H., Cao, C., Hao, C.-N., Liu, F.-S., Wang, J.-L., Xia, X.-Y., Deng, Z.-G., & Young, C. K.-S. 2005, ApJ, 632, L79
Yan, L., McCarthy, P.J., Freudling, W., Teplitz, H.I., Malumuth, E.M., Weymann, R.J., & Malkan, M.A. 1999, ApJ, 519, L47